SCIENCE CHINA Materials

REVIEWS

mater.scichina.com link.springer.com

Published online 17 March 2015 | doi: 10.1007/s40843-015-0037-2
Sci China Mater 2015, 58: 241–257

Mesoporous carbon biomaterials

Yu Chen* and Jianlin Shi*

Nano-biotechnology provides highly efficient and versatile strategies to improve the diagnostic precision and therapeutic efficiency of serious diseases. The development of new biomaterial systems provides great opportunities for the successful clinical translation of nano-biotechnology for personalized biomedicine to benefit patients. As a new inorganic material system, mesoporous carbon biomaterials (MCBs) combine the merits of a mesoporous nanostructure and carbonaceous composition, showing superior qualities compared with traditional mesoporous silica and other carbon-based nanosystems, such as graphene, carbon nanotubes, and fullerene. Thus, this review focuses on the rational design, chemical synthesis, and biomedical applications of MCBs. The synthetic strategies for MCBs, especially mesoporous carbon nanoparticles (MCNs), are summarized, and several representative biomedical applications of MCBs are discussed in detail. MCBs perform well for on-demand drug-release, photothermal therapy, synergistic therapy, fluorescent labeling of cancer cells, bio-adsorption of *in vivo* toxic pathogenic substances, peptide separation, and biosensing. The preliminary biosafety issue of MCBs is also briefly discussed. Finally, the critical issues and challenges facing the future development of MCBs for clinical translation are considered. There is great promise for MCBs to reach clinical translations for biomedical applications based on their unique nanostructure, composition, and biocompatibility once some critical issues are fully addressed.

INTRODUCTION

Carbon-based materials are an emerging focus in the material science community and have received great attention for their high performance in extensive applications due to their unique structure and distinctive physiochemical properties and biological behaviors such as high chemical inertness/mechanical stability, excellent electrical conductivity, and satisfactory biocompatibility [1–3]. Of the carbon-family members, sp^2 carbon-based materials such as fullerene [4,5], carbon nanotubes [1,6–11], carbon dots [12–14], and graphene [15–18], have been explored for promising applications in biomedicine, including drug delivery, gene transfection, photothermal therapy, photodynamic therapy, biosensing, and even tissue engineering [19–21]. For instance, the hollow space in fullerene/carbon nanotubes and large surface-to-volume ratio of graphene can be used for the encapsulation and intracellular delivery of therapeutic agents. Moreover, carbon nanotubes and graphene show enhanced laser absorption in the near-infrared (NIR) region and high photothermal-conversion efficiency and can act as photothermal agents for photothermal cancer therapy. Pre-clinical evaluations of biodistribution, excretion, histocompatibility, hemocompatibility, and other properties are very encouraging: sp^2 carbon-based biomaterials are nontoxic and biocompatible at adequate doses, showing high clinical-translation potential [20,22,23].

Biocompatible inorganic mesoporous materials have attracted great attention in biomedicine over the past decades [24–28]. The well-defined mesoporous structures with large surface area, high pore volume, and tunable pore sizes provide large reservoirs for guest molecules and show sustained drug-release profiles [29–31]. Mesoporous silica nanoparticles (MSNs) are one of the most representative and explored mesoporous biomaterials in biomedicine due to their high biocompatibility, tunable biodegradation, sustained drug-releasing performance, and easy surface modifications (Fig. 1) [32–35]. Compared with traditional MSNs and other carbon-based nanosystems (e.g., carbon nanotubes, graphene, carbon nanodots, and fullerene), mesoporous carbon biomaterials (MCBs), especially mesoporous carbon nanoparticles (MCNs), have been rarely used for biomedical applications, probably due to the lack of adequate synthetic methodologies to fabricate MCNs with desirable composition, dimension, structure, dispersity, and physiochemical properties for biomedicine. Typically, MCBs fabricated by conventional nanocasting methods possess irregular morphology and large particulate size, usually in the range of several micrometers. Furthermore, such MCBs are inherently hydrophobic, which severely restricts their potential applications in biomedicine where hydrophilic nanoparticles are highly desirable for intravenous injection and blood-vessel circulation. Compared with one-dimensional (1D) carbon nanotubes and two-dimensional (2D) graphene, quasi-zero-dimensional (0D) MCNs with spherical morphology facilitate the free

State Key Laboratory of High Performance Ceramic and Superfine Microstructures, Shanghai Institute of Ceramics, Chinese Academy of Sciences, Shanghai 200050, China
* Corresponding authors (emails: chenyu@mail.sic.ac.cn (Chen Y); jlshi@mail.sic.ac.cn (Shi J))

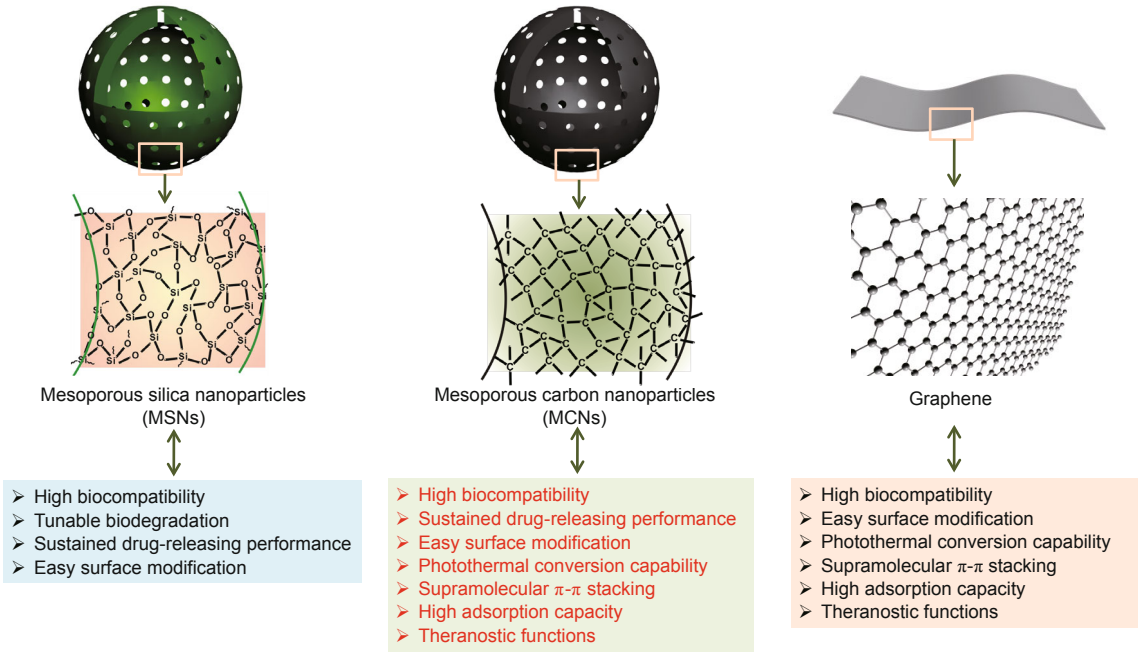

Figure 1 Schematic illustrations of the structure and framework composition of MSNs, MCNs and graphene and their individual unique characteristics in biomedical applications.

transport of loaded agents within blood vessels. Notably, MCBs show high biocompatibility, sustained drug-releasing behavior, easy surface modification, high photothermal-conversion efficiency, specific supramolecular π-π stacking with aromatic-drug molecules and some unique theranostic functions, i.e., MCBs combine the advantages of mesoporous nanostructure and carbonaceous composition. Therefore, they are considered the next generation of mesoporous materials and carbon biomaterials in biomedicine. It is anticipated that MCBs could be extensively applied in biomedicine if the above-mentioned critical issues (e.g., irregular morphology, large particle size, hydrophobicity, etc.) are satisfactorily solved.

This review focuses on typical chemical-construction strategies of MCBs for various biomedical applications, including nanocasting, soft-templating, and *in situ* framework transformation. Methods for surface engineering as-synthesized carbon biomaterials, which are necessary for *in vivo* translations, are also included. This review discusses the biomedical performances of various MCBs in drug delivery, photothermal therapy, synergistic therapy, cell labeling, removal of toxic pathogenic substances, capture of peptides from biosamples, and biosensing. Preliminary biosafety evaluations are also briefly discussed.

SYNTHETIC APPROACHES FOR MESOPOROUS CARBON MICRO/NANOPARTICLES

The broad applications of MCBs motivate the fast development of diverse chemical synthesis strategies such as soft-/hard-templating approaches and *in situ* framework transformation to prepare MCBs with desirable compositional/structural features. To fabricate desirable MCBs for specific biomedical applications, a rational choice of adequate synthetic strategy is crucial.

Nanocasting

The earliest and one of the most frequently adopted strategies to fabricate mesoporous carbon materials was based on the nanocasting process, generally using as-synthesized mesoporous silica as the host template [36]. Typically, mesoporous silica is synthesized as a hard template, followed by the impregnation and infiltration of organic carbon sources. Polymerization/carbonization of carbon sources at high temperature and removal of the silica template by chemical etching then produces ordered mesoporous carbon [37]. Based on the nanocasting method, Kim *et al.* [38] constructed spherical MCNs with ordered mesoporous structures using MCM-48 MSNs as the hard template. The average particle size of as-synthesized MCNs was ~150 nm. However, the traditional nanocasting method encounters severe problems in the fabrication of hydrophilic MCNs with uniform spherical morphology and high dispersity. Excess deposition of the carbon precursor on the outside of the silica templates is difficult to remove during the casting process, and a washing step would also remove the organic carbon precursor within the mesopores. Moreover,

high-temperature calcination to carbonize the carbon precursor results in the hydrophobicity of MCNs.

To fabricate hydrophilic MCNs with high dispersity via the nanocasting method, we recently presented a facile hydrothermal-synthetic protocol to fabricate MCNs with uniform spherical morphology [39]. MCM-48 MSNs were initially functionalized with amino groups to generate positively charged $-NH_3^+$ ions on the mesopore surface. Negatively charged carbonaceous polysaccharide (PS) from glucose aqueous solution under hydrothermal conditions was attracted to the mesopore surface via electrostatic interaction between PS molecules and the pre-established $-NH_3^+$ ions. This amino-functionalization step avoided heterogeneous formation of carbon spheres on the outside of the MCM-48 template. The obtained MCNs could be well dispersed into aqueous solution with a hydrodynamic size of ~240 nm. A general confined co-assembly strategy was recently established to fabricate highly uniform mesoporous carbon microspheres employing three-dimensional (3D) ordered macroporous silica as the hard template [40]. These mesoporous carbon spheres range in size from 0.8 to 1 μm; however, the large particle sizes limit their utilization in intravenous drug delivery and diagnostic imaging.

Soft-templating

MCNs synthesized by the nanocasting method inversely duplicate the structure of hard templates; thus, their microstructure and morphology are limited to those of the initial templates. Additionally, aggregation of MCNs is intrinsically difficult to avoid in the traditional nanocasting process. Recent advances in synthetic chemistry allowed synthesis of mesoporous carbon materials with ordered mesoporosity using a soft-templating method, i.e., organic-organic co-assembly strategy. For instance, amphiphilic triblock copolymers could serve as the soft template to self-assemble with resorcinol-formaldehyde resin to fabricate ordered mesoporous carbon materials [41,42]. However, controlling the morphology and particle-size distribution of mesoporous carbon is difficult in traditional soft-templating synthesis. To solve this critical issue, Fang *et al.* [43] recently developed a low-concentration hydrothermal process to synthesize MCNs with ordered body-centered mesoporosity, spherical morphology, and narrow size distribution. Hydrogen bonding between Pluronic F127 ($EO_{106}PO_{70}EO_{106}$; EO: ethylene oxide, PO: propylene oxide) and resols promoted the formation of spherical phenolic resol-F127 monomicelles (Fig. 2a). The low concentration of reactants was necessary to avoid excessive cross-linking among as-formed monomicelles. After hydrothermal treatment, the monomicelles assembled to generate the mesostructure by cross-linking with phenolic resols. MCNs were finally produced by further high-temperature calcination under N_2 protection. The achieved MCNs feature highly ordered mesoporosity and uniform spherical morphology (Figs 2b and c). Importantly, the particle sizes of MCNs can be precisely tuned from 20 to 140 nm by changing the initial reagent concentrations. However, the low precursor concentration in this method is a strong limiting factor for the large-scale synthesis of MCNs and is thus unfavorable for industrial translations.

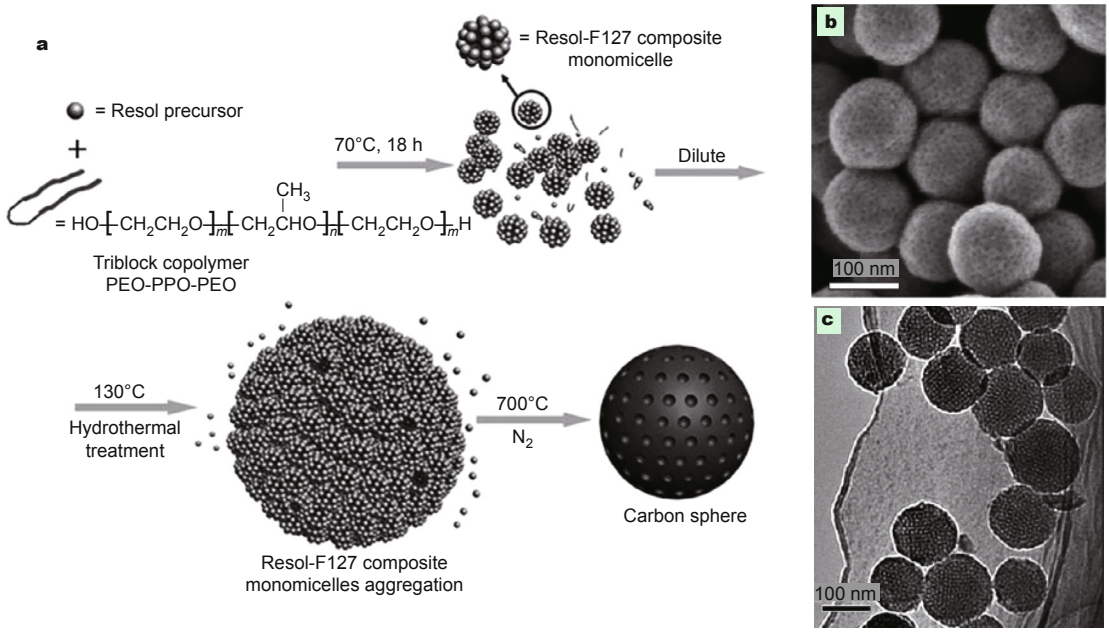

Figure 2 (a) Schematic illustration of the soft-templating synthetic mechanism of MCNs. (b) SEM and (c) TEM images of 140-nm MCNs. Reprinted with permission from Ref. [43]. Copyright 2010, WILEY-VCH Verlag GmbH & Co. KGaA.

For the large-scale synthesis of MCNs with uniform spherical morphology and high dispersity, Liu *et al.* [44] reported the synthesis of ordered mesoporous resorcinol formaldehyde nanospheres by employing the cationic fluorocarbon surfactant FC4 ($C_3F_7O(CFCF_3CF_2O)_2CF$-$CF_3CONH(CH_2)_3N^+(C_2H_5)_2CH_3I^-$) and triblock copolymer Pluronic F127 as the soft templates. Resorcinol and formaldehyde (RF) were used as organic carbon precursors to assemble with soft templates via hydrogen bonding (Fig. 3). After further carbonization of as-synthesized polymer spheres, 80–400 nm MCNs were successfully synthesized. For MCNs with large pores, Tang *et al.* [45] synthesized nitrogen-doped MCNs with concurrent large (16 nm) mesopores and small (200 nm) particle sizes by self-polymerization of dopamine and co-assembly with a high-molecular-weight diblock polymer PB-*b*-PEO. The soft-templating strategy features controllable MCN morphology. For instance, well-controlled MCN shapes from sphere to rod were obtained by using low-molecular-weight phenolic resol as the carbon source and triblock copolymer Pluronic F127 as the structure-directing agent, with the concentration of F127 determining the resultant MCN morphology [46]. Thus, the particle size, pore size, and morphology of MCNs can be easily controlled by selecting adequate synthetic parameters for the soft-templating approach.

The soft-templating approach can also produce mesoporous carbon with concurrent uniform spherical morphology and extra-large particle sizes. We recently presented a novel emulsion-EISA (evaporation-induced self-assembly) strategy to fabricate uniform spherical mesoporous carbon with the sizes in the millimeter range for *in vitro* blood purification by hemoperfusion [47]. Triblock copolymer Pluronic F127 and phenolic resols were dissolved in ethanol, and the solution was dispersed in oil to form emulsion droplets (Fig. 4a). The co-assembly of Pluronic F127 and phenolic resols tended to form mesophase hybrids upon the evaporation of ethanol. The as-formed primary droplets fused with surrounding droplets to form very large polymer particles during thermal polymerization. After carbonization of the polymer particles, extra-large mesoporous carbon spheres (1.08–1.90 mm) were formed (Fig. 4b). The mesopores of these carbon particles are disordered and worm-like (Fig. 4c), and SEM images (Figs 4d and e) showed that these millimeter-sized mesoporous carbon particles had smooth surfaces. This research provides direct evidence that the soft-templating approach can synthesize spherical mesoporous carbon particles with a wide range of sizes.

In situ framework transformation

Traditional nanocasting using hard templates is time consuming and tedious because of the multi-step infiltration and post treatments. Particle aggregation and hydrophobicity are the two critical issues to be solved. Toward addressing these concerns, we recently developed a new *in situ* framework transformation strategy to synthesize hollow MCNs (HMCNs) with large hollow interiors and unique red blood cell (RBC) morphology [48]. Mesoporous organosilica nanoparticles (MONs) were initially synthesized with benzene-bridged organic-inorganic hybrid frameworks [49]. High-temperature calcination of mesoporous organosilica carbonizes the organic-benzene groups to form a mesoporous carbon framework within the silica framework. Upon removing the silica component by chemical etching, uniform HMCNs with RBC morphology were obtained (Figs 5a and b). Because the as-formed carbonaceous framework is not rigid enough to maintain the spherical and hollow nanostructure after removal of the silica component, most of the mesoporous carbon shell

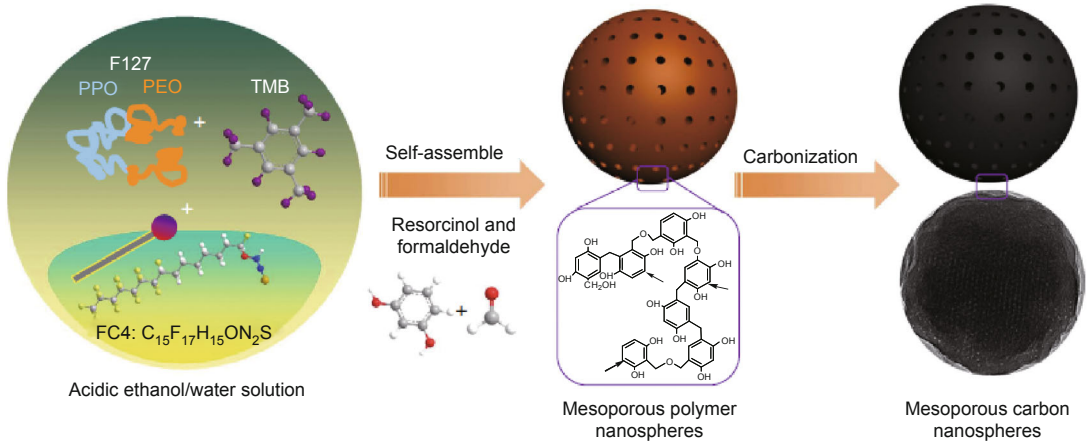

Figure 3 Schematic illustration of the fabrication of mesoporous polymer and MCNs. Reprinted with permission from Ref. [44]. Copyright 2013, Nature Publishing Group.

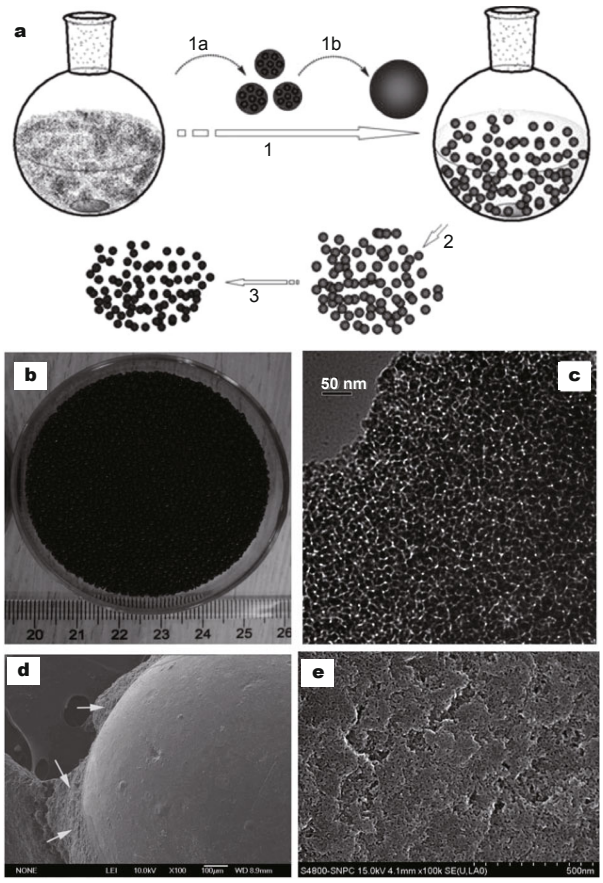

Figure 4 (a) Schematic illustration of the formation of millimeter-sized mesoporous carbon particles. (b) Photographic, (c) TEM, and (d, e) SEM images of as-obtained mesoporous carbon particles. Reprinted with permission from Ref. [47]. Copyright 2010, Royal Society of Chemistry.

collapses into the hollow interior to produce RBC morphology (Figs 5c and d).

MCNs, HMCNs, and rattle-type MCNs were recently synthesized using a "silica-assisted" synthetic strategy [50]. The polymerization of phenolic resols and hydroxylation/condensation of tetraethylorthosilicate (TEOS) could form the organic-inorganic hybrid framework of composite nanoparticles. After further carbonization and removal of the silica component, highly dispersed MCNs with either solid or hollow nanostructures were obtained. Interestingly, the hollow nanostructure of MCNs was tuned by changing the initial precursor ratios of phenolic resols and TEOS [50]. Compared with the traditional nanocasting method, the *in situ* framework-transformation strategy is easy and scalable and is considered as a non-conventional method to fabricate MCNs with desirable key parameters.

Surface modification

The carbonaceous framework of MCNs is generally formed by calcination or hydrothermal treatment at elevated temperatures. Therefore, pristine MCNs are almost hydrophobic, which is unfavorable for broad biomedical application. Oxidization MCNs using a concentrated strong acid (e.g., HNO_3 and H_2SO_4) is the most adopted strategy to improve their hydrophilicity [51]. This acid treatment can also modify the surface of MCNs with abundant functional groups (e.g., carboxyl groups) for further organic modifications such as PEGylation, targeting, stimuli-responsive grafting, diagnostic-imaging multifunctionalization, etc.

Hyaluronic acid (HA) was grafted onto the surface of MCNs to improve their colloidal stability/biocompatibili-

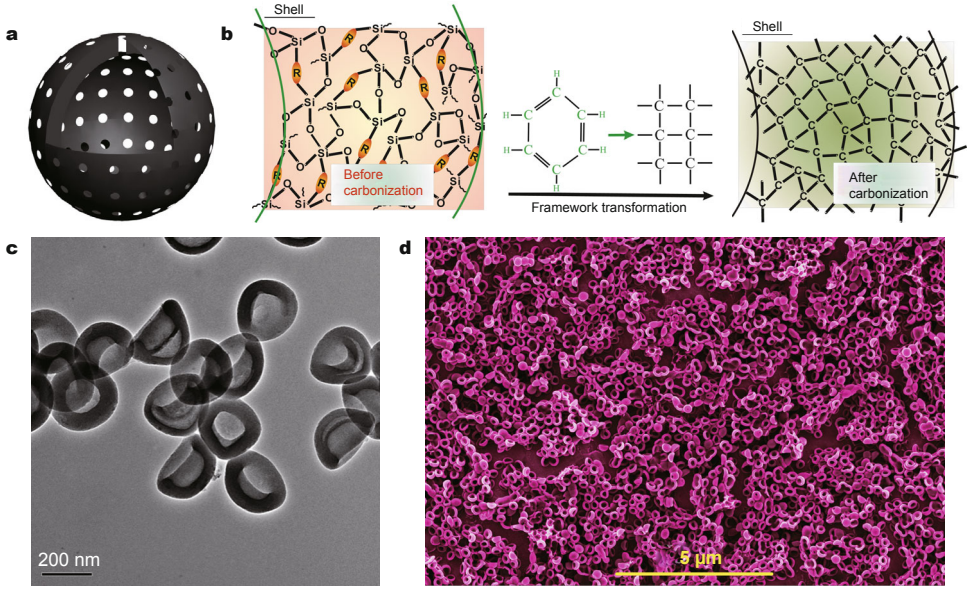

Figure 5 (a) Schematic illustration of HMCNs and (b) the *in situ* framework transformation from benzene-bridged organosilica to a carbonaceous framework. (c) TEM and (d) SEM images of oxidized HMCNs. Reprinted with permission from Ref. [48]. Copyright 2014, WILEY-VCH Verlag GmbH & Co. KGaA.

ty and endow the carrier with CD44-targeting capability [52]. After oxidization of MCNs in a mixture of concentrated HNO_3 and H_2SO_4, MCNs were modified with hyper-branched polyethylenimine (PEI) via carbodiimide coupling [53]. Folic acid (FA) was further linked to the surface of PEI-modified MCNs by reaction of the PEI amino group with the FA carboxyl group. FA modification of MCNs was effective in targeting HeLa cells with overexpressed folate receptors. For on-demand drug release, CMK-3 surfaces were modified with poly(*N*-isopropyl acrylamide) (PNIPAM) by *in situ* polymerization of PNIPAM [54]. The temperature-responsive nature of PNIPAM permitted thermo-sensitive drug-releasing behavior of PNIPAM-modified CMK-3 with a pronounced transition at 20–25°C.

BIOMEDICAL APPLICATIONS OF MCBS

The unique mesoporous nanostructure and carbonaceous composition of MCBs endow them with high biomedical performance. Similar to MSNs, the well-defined mesopores can provide reservoirs for guest drug molecules, and the carbonaceous framework and NIR-absorption property of MCBs can be used for photothermal conversion and therapy. The high absorption capability of MCBs shows the potential for application in bio-adsorption of toxic pathogenic substances and separation of peptides. The unique structural/compositional and physiochemical property of MCBs can be used to construct biosensing platforms.

MCBs for controlled delivery and release of therapeutic agents

MCNs are suitable for drug delivery because they allow hydrophobic interactions and supramolecular π-π stacking between the drug molecules and carbonaceous framework. Importantly, such non-covalent interactions are very sensitive to external triggers, which can be used to construct intelligent nanosystems with on-demand drug release. In addition, the well-defined mesopores serve as the storage reservoirs and diffusion path for guest molecules. The nanosized mesopores in MCNs can also reduce the drug-release rate, exhibiting sustained releasing behavior. Importantly, the tunable particle size and spherical morphology endow MCNs with intravenous transport capability. Therefore, MCNs can be regarded as one of the most promising carriers for efficient drug delivery.

Kim *et al.* [38] synthesized CMK-1 MCNs via nanocasting using MCM-48 MSNs as the hard template. Fura-2 membrane-impermeable fluorescent dye molecules were encapsulated within MCNs for transmembrane delivery in human cancer cells (Fig. 6a). The small particle size allowed MCNs to enter cells via a general endocytosis path, which was similar to most reported nanosystems. Differential interference contrast (DIC) microscopic images along the *Z*-axis of HeLa cells after co-incubation with MCNs (24 h) showed that MCNs were successfully internalized into the cells (Figs 6b–d). Fura-2-loaded MCNs exhibited a sustained intracellular Fura-2 release profile. These results indicate that MCNs could act as transmembrane vectors for the delivery of loaded cargoes. However, the fabricated MCNs aggregate in aqueous solution due to their hydrophobicity after carbonization of furfuryl alcohol at elevated temperature. Compared to traditional MSNs, MCNs are much more suitable for the encapsulation and delivery of hydrophobic therapeutic agents because the carbonaceous

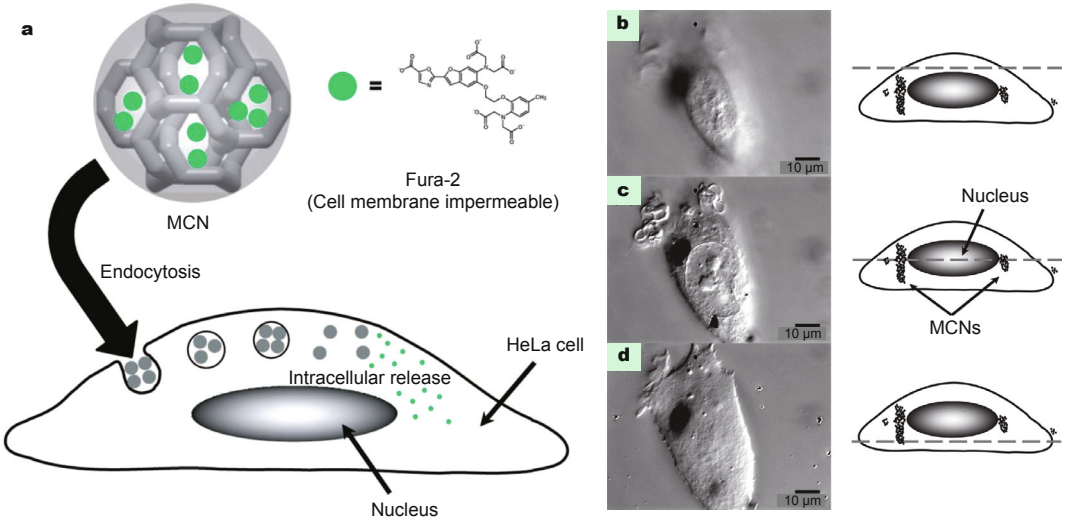

Figure 6 (a) Schematic illustration of Fura-2-loaded MCNs for transmembrane delivery and intracellular release of Frua-2. (b–d) Optical images (left) and schematic illustrations (right) of HeLa cells after co-incubation with MCNs. The images were obtained by varying the focal plane along the *Z*-axis from the (b) top, (c) middle, and (d) bottom of the cells. Reprinted with permission from Ref. [38]. Copyright 2008, American Chemical Society.

framework of MCNs can form specific π-π supramolecular interactions with aromatic drug molecules. We recently demonstrated that the as-synthesized MCNs showed loading capacity as high as 17% for the hydrophobic anticancer drug camptothecin (CPT) [39], substantially higher than those of MSN-based nanocarriers [55]. Mesoporous carbon also exhibits a sustained release profile for an analgesic drug (antipyrine) [56].

The carbonaceous framework of HMCNs can form supramolecular π-π stacking interactions with aromatic drug molecules [17,48]. We recently demonstrated that the anticancer drug doxorubicin (DOX) could be firmly anchored within mesopore channels of HMCNs by such π-π stacking interactions (Fig. 7a), which could be disrupted by pH changes (Fig. 7b) or focused ultrasound irradiation (Fig. 7c) [48]. For instance, the DOX-releasing amount was as low as 3.65% over 24 h in pH 7.4 buffer solution but increased to 12.51% and 37.61% in pH 6.0 and 4.6 solutions, respectively (Fig. 7b). Because the microenvironment of tumor tissue is more acidic than normal tissue [15,57–60], this pH-responsive DOX-releasing profile facilitates tumor-localized drug release from HMCNs. Focused ultrasound could also break the π-π stacking to trigger the DOX release. Furthermore, DOX release exhibited a pulsatile profile with pulses of high-intensity focused ultrasound (HIFU) irradiation (Fig. 7c). This on-demand drug-release pattern is of practical importance because the focused ultrasound noninvasively penetrates to deep tumors [61–63]. As expected, HMCN-mediated DOX delivery significantly enhanced the therapeutic efficiency and sustainably inhibited tumor growth compared to free DOX (Fig. 7d). Similar pH-dependent DOX release from 90-nm MCNs was also demonstrated at pH 5.5, 7.4, and 9.0 [51].

MCNs based core/shell composites show promise for desirable drug-loading/releasing patterns. Thus, MCNs were coated with a layer of mesoporous silica (designated

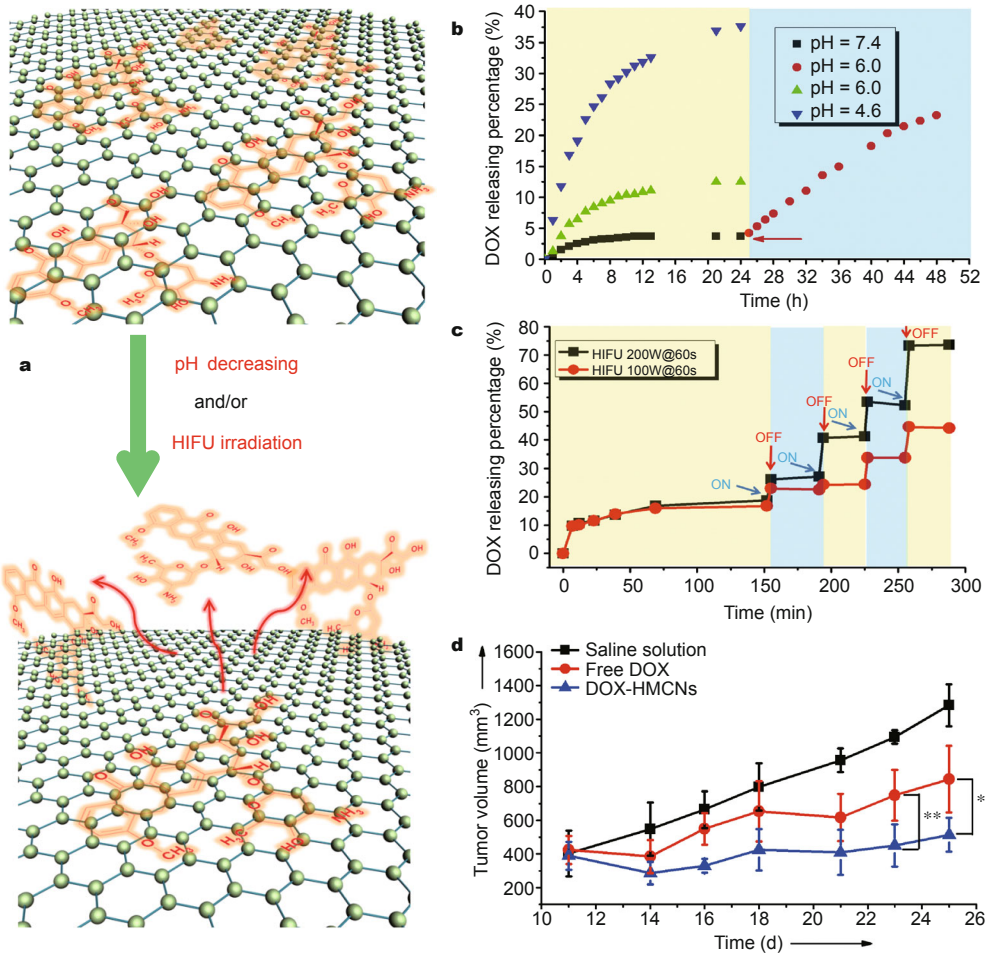

Figure 7 (a) Schematic illustration of the supramolecular π-π stacking between carbonaceous framework of MCNs and aromatic DOX molecules. (b) pH- and (c) HIFU-responsive drug release. (d) Tumor-growth curves for tumor-bearing mice after treatment with free DOX and DOX-HMCNs. Reprinted with permission from Ref. [48]. Copyright 2014, WILEY-VCH Verlag GmbH & Co. KGaA.

as mesoporous carbon@mesoporous silica, MC@MS) for the co-delivery of hydrophilic (cisplatin) and hydrophobic (paclitaxel, Ptxl) anticancer agents [64]. A unique hollow cavity was created between the mesoporous carbon core and mesoporous silica shell (Figs 8a and b) via thermal treatment. The hydrophobic MCNs show high affinity for water-insoluble anticancer agents, while the hydrophilic mesoporous silica shell attracts water-soluble agents (Fig. 8c). The co-delivery of dual anticancer agents achieved synergistic therapeutic outcomes, efficiently killing both the normal ovarian cancer cells (SKOV3, Fig. 8d) and drug-resistant A2780 cancer cells (Fig. 8e).

To further control DOX release, HA was included as a gatekeeper to seal DOX within the mesopores of MCNs with a redox-responsive disulfide bond [52]. Upon the addition of enzyme Hyal-1, HA was degraded into low-molecular-weight fragments, triggering DOX release. Reducing agents such as GSH or DTT can break the disulfide bonds to remove the HA gatekeeper, substantially accelerating DOX release. Additionally, mesoporous carbon was employed as a carrier to enhance the inhibitory effect of celecoxib on the metastasis of MDA-MB-231 cells as demonstrated by wound healing, migration, and invasion analyses [65]. We recently demonstrated that HMCNs themselves significantly inhibit cancer cell metastasis by silencing the expressions of metastasis-promoting proteins such as matrix metalloproteinase MMP9, cyclo-oxygenase-2 (COX-2), and urokinase-type plasminogen activator (uPA) proteins [48]. Moreover, MCNs with large mesopores are effective adjuvants for efficient *in vivo* oral vaccine delivery [66]. To encapsulate biomacromolecules, magnetic mesoporous carbon spheres with dual mesopore structure were synthesized for the loading and sustained release of an antibacterial enzyme [67].

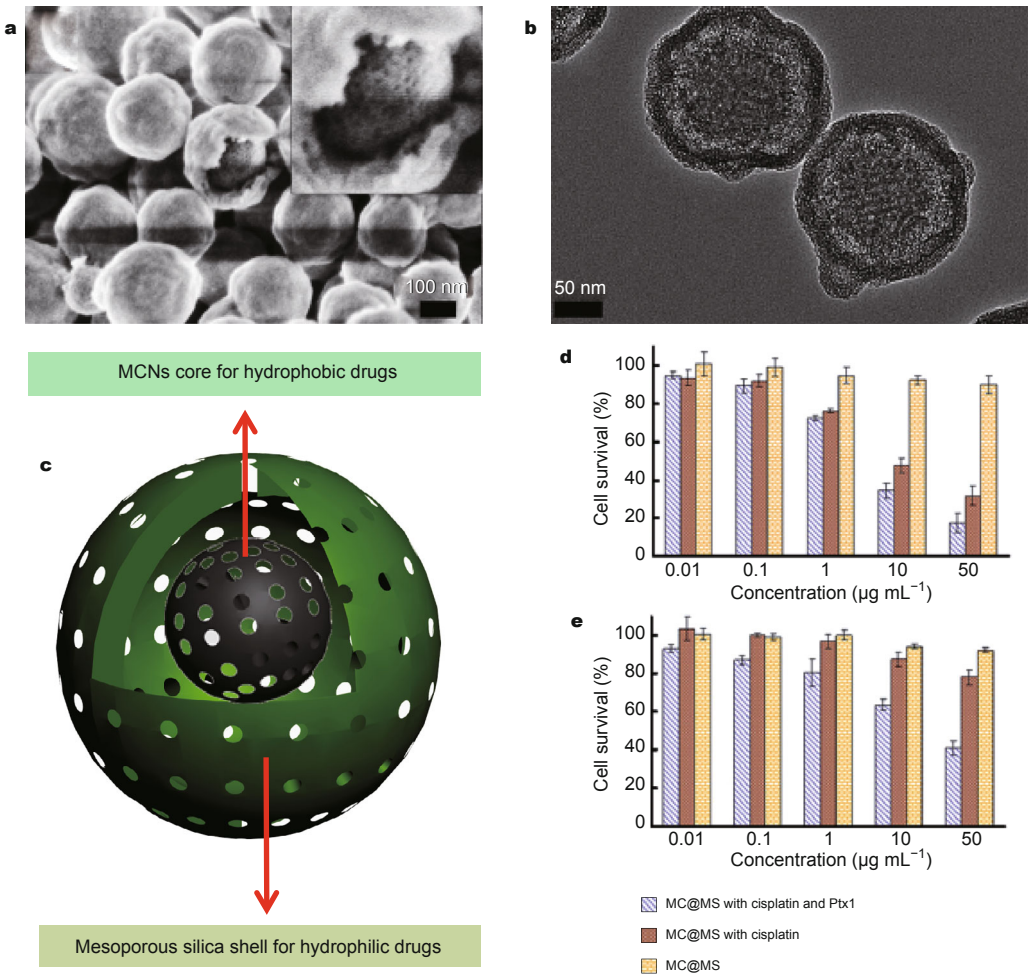

Figure 8 (a) TEM and (b) SEM images of MC@MS rattle-type nanoparticles. (c) Schematic illustration of the co-encapsulation of hydrophobic and hydrophilic anticancer agents within MC@MS. *In vitro* cytotoxicity of (d) normal SKOV3 ovarian cancer cells and (e) drug-resistant A2780 (CP70) cells by co-incubation with cisplatin and paclitaxel (Ptxl) co-loaded MC@MS (gray), cisplatin-loaded MC@MS (brown), and MC@MS (yellow). Reprinted with permission from Ref. [64]. Copyright 2014, WILEY-VCH Verlag GmbH & Co. KGaA.

MCBs for photothermal and synergistic therapy

Similar to carbon nanotubes and graphene [68–72], MCNs show strong optical absorption in the NIR region (e.g., 808 nm), indicating potential utility as the photothermal agent for photothermal ablation of cancer cells because NIR light penetrates deeply into tissues and is harmless to normal tissues [52,53]. Xu *et al.* [53] recently demonstrated that FA-targeted MCNs showed superior photothermal-conversion efficiency compared to graphene oxide and showed that NIR irradiation accelerated the release of pre-loaded anticancer drugs from MCNs. In addition, HA-targeted MCNs (MCNs-HA) were designed for targeted photothermal ablation of tumor and synergistic on-demand drug release [52]. MCNs-HA targeted to CD44 overexpressed cell membranes and entered the cancer cells, and then DOX release was triggered and accelerated by NIR irradiation. Thus, NIR irradiation played two roles: it was the source for photothermal conversion to ablate the cancer cells and the trigger for DOX release from MCNs. NIR-based photothermal therapy and DOX-based chemotherapy substantially enhanced the therapeutic efficiency, as demonstrated by the *in vitro* CCK-8 assay [52].

The combination of carbon and silica components could produce mesoporous composite materials with high photothermal conversion efficiency and controlled drug-releasing performance. Semi-graphitized carbon was introduced *in situ* to the mesopores of MSNs for concurrent photothermal therapy and drug delivery [73]. Wang *et al.* [74] designed an MCN core/mesoporous silica shell nanosystem. The hydrophilic mesoporous silica shell was used for surface modification to guarantee hydrophilicity and targeted drug delivery, and the hydrophobic graphitic mesoporous carbon core facilitated the encapsulation of hydrophobic drugs and NIR-induced photothermal therapy. DOX-loaded graphitic carbon@silica nanospheres exhibited pH-responsive drug-release profiles, and the introduction of NIR irradiation accelerated DOX release (Fig. 9a). Treatment of SK-BR-3 with bafilomycin A1 to inhibit lysosome acidification and elevate the intralysosomal pH significantly inhibited the release of DOX from the carrier, as demonstrated by decreased DOX fluorescence within cancer cells (Figs 9b–e). Therefore, intracellular DOX release was also pH-dependent. The synergistic therapeutic outcome of photothermal therapy and chemotherapy was further demonstrated *in vitro*.

NIR irradiation of the unique sp^2 and sp^3 carbonaceous structure of MCNs can produce additional cellular reactive oxygen species (ROS) and persistent free radicals, which further generates a large number of heat shock factor-1 protein homotrimers to suppress the activation and function of resistance-related proteins and genes (e.g., expression of MDR-1 and TP53 genes) in multidrug-resistant (MDR) cancer cells (Fig. 10) [75]. NIR-induced free radical generation by HMCNs was attributed to three factors. First, the electronic and chemical properties of HMCNs catalyze the oxidation of small molecules and produce ROS. Second, laser irradiation changes the features of HMCNs and the cancer cell microenvironment, which enhances electron transport within the cancer cells. Third, NIR irradiation destroys lysosomal membranes, releasing HMCNs into the cytoplasm and facilitating the catalysis of small molecules to generate more free radicals. Concurrent NIR-triggered free radical generation and DOX delivery can have synergistic therapeutic effects to combat MDR cancer cells.

MCBs for bio-imaging, bio-adsorption, and biosensing

Carbon dots and graphene quantum dots (QDs) have been extensively explored for cell labeling [76–82]. Using rational structural/compositional design, MCBs can be endowed with fluorescent properties for bio-imaging. Our

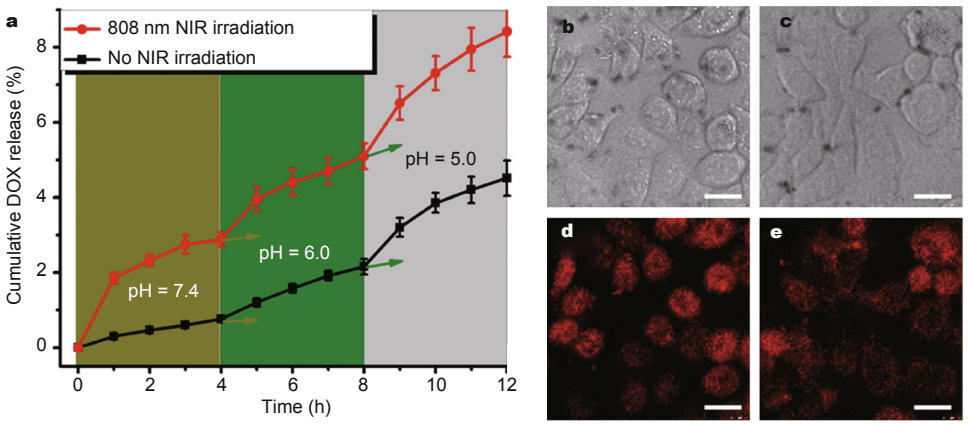

Figure 9 (a) DOX-releasing profile from graphitic carbon@silica nanospheres. (b–e) Optical microscopic images of cells after pH-triggered release of DOX (red in d and e) from the carrier in SK-BR-3 cells. The cells were treated without (b, d) and with (c, e) bafilomycin A1. Scale bar = 20 μm. Reprinted with permission from Ref. [74]. Copyright 2014, American Chemical Society.

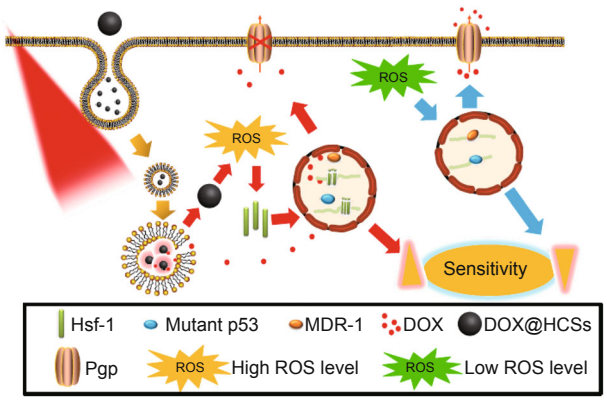

Figure 10 Schematic illustration of reversing the multidrug resistance (MDR) of cancer cells employing HMCNs (expressed as HCSs in the scheme) as the DOX carrier and ROS generator under laser irradiation. Reprinted with permission from Ref. [75]. Copyright 2015, American Chemical Society.

group recently synthesized fluorescent MCNs (F-MCNs) using a facile precursor carbonization-in-hot-solvent route [83]. Citric acid was decomposed and carbonized in 1-octadecane at 240°C to form ~100-nm F-MCNs with well-defined mesoporous structures and BET surface area of 864 $m^2 g^{-1}$, pore volume of 0.91 $cm^3 g^{-1}$, and average pore size of 2.7 nm. Notably, F-MCNs exhibited multicolor and upconversion photoluminescence (Figs 11a and b), which was similar to reported characteristics of carbon dots with multicolor and wavelength-dependent fluorescence emissions upon laser excitation at different wavelengths. The F-MCNs showed photoluminescence efficiency up to 37%. Confocal laser scanning microscopic (CLSM) images showed that F-MCNs could illuminate cancer cells after endocytosis (Figs 11c–e). The cell-labeling fluorescence was also photo-stable, potentially superior to organic fluorescein, which has relatively low photostability. The upconversion-photoluminescence cell labeling was demonstrated by green fluorescence emission after excitation at 637 nm (Fig. 11e). Additionally, the well-defined mesoporosity of F-MCNs could act as a reservoir for the encapsulation and intracellular delivery of therapeutic agents, thereby serving as a theranostic agent.

For mesoporous carbon/silica composite nanoparticles, we recently integrated carbon components within the mesopores of mesoporous silica by directly carbonizing intra-mesopore P123 surfactant micelles (Fig. 12) [84]. We further created oxygen vacancies within the silica frame-

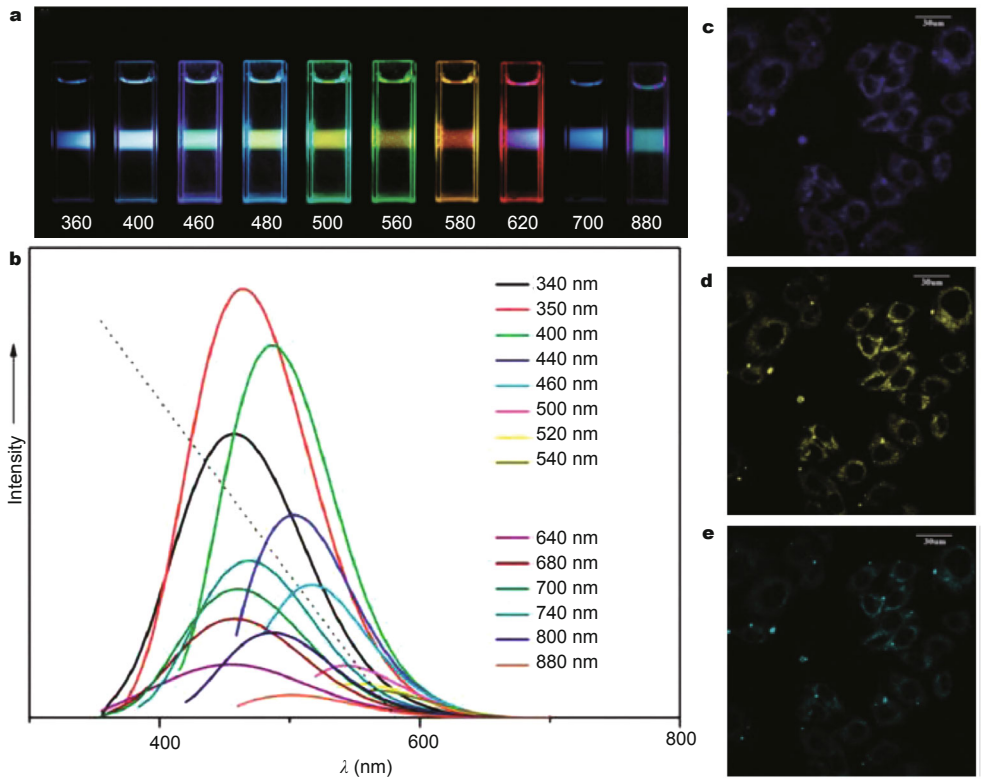

Figure 11 (a) Photographs and (b) photoluminescent spectra of F-MCNs in aqueous solution under laser excitation at different wavelengths. (c–e) CLSM images of HeLa cells labeled with MCNs (c: λ_{ex} = 340 nm, detected using a 425–475 nm long-pass filter; d: λ_{ex} = 488 nm, detected using a 520–560 nm long-pass filter; e: λ_{ex} = 637 nm, detected using a 425–475 nm long-pass filter). Reprinted with permission from Ref. [83]. Copyright 2014, Royal Society of Chemistry.

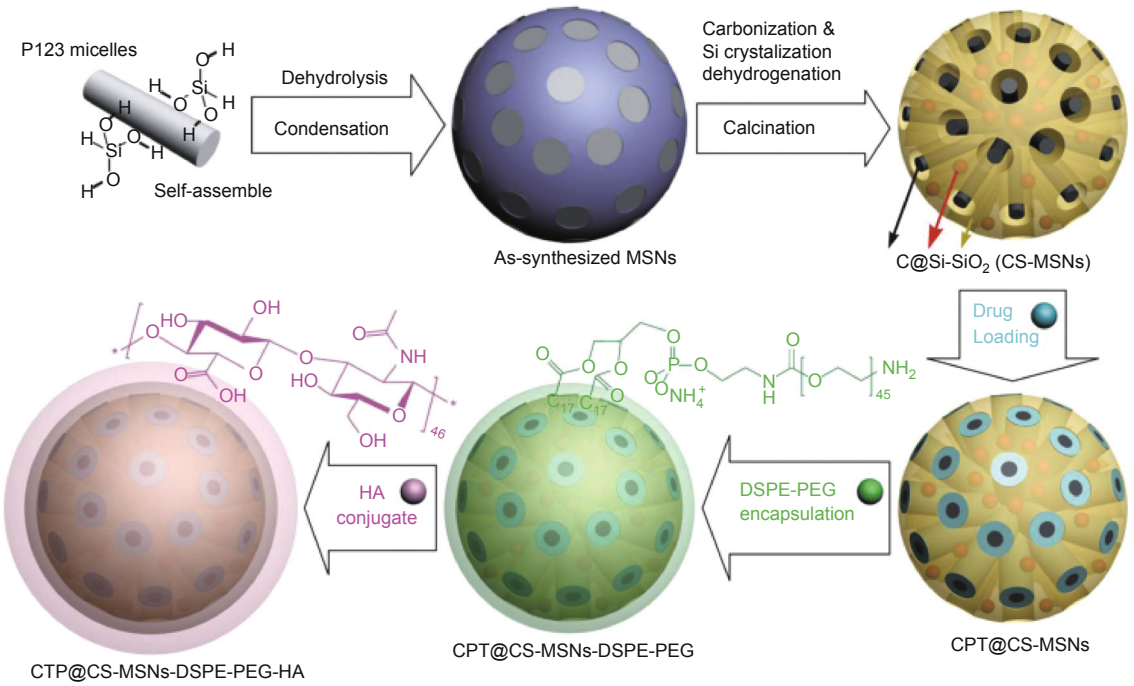

Figure 12 Schematic illustration of the synthesis of fluorescent mesoporous carbon/silica composite nanoparticles, subsequent CPT encapsulation, and surface modification. Reprinted with permission from Ref. [84]. Copyright 2012, Elsevier.

work by dehydrogenation between O_3Si-H terminal groups at 600°C. Hybridization of C and Si nanocrystals within the framework could endow MSNs with unique characteristics for biomedical applications: the confined carbon component within the mesopores increases the loading capacity for a hydrophobic anticancer agent (camptothecin, CPT), and the confined Si nanocrystals within the framework present unique NIR-to-visible luminescence for cell labeling. Based on these characteristics, this composite nanocarrier is promising for the delivery of water-insoluble therapeutic agents and cancer theranostics. Furthermore, MCNs could be covalently grafted with fluorescein (e.g., 6-aminofluorescein) to study endocytosis by confocal fluorescent imaging [85].

Mesoporous carbon possesses a high adsorption capacity for various guest molecules [86–89]. In addition, their excellent biocompatibility and chemical/mechanical stability allow them to adsorb toxic pathogenic substances *in vivo*. We demonstrated that HMCNs could act as a clinical adsorbent for bilirubin [90], which can cause crippling, athetoid cerebral palsy and even death if overproduced [91]. Various absorbents such as activated carbon, chitosan, resins, and porous TiO_2 have been employed as adsorption materials in hemoperfusion columns to remove bilirubin from the blood [90]. HMCNs with large hollow interiors and well-defined mesoporous shells (Figs 13a and b) were elaborately synthesized using silica core/mesoporous silica shell core/shell-type templates and exhibited substantially higher bilirubin-adsorption capacity (304 mg g^{-1}) compared with commercial activated carbon (70 mg g^{-1}) and CMK-3 mesoporous carbon (198 mg g^{-1}). This high bilirubin-adsorption capacity (Figs 13c and d) was attributed to the large hollow interior and well-defined mesopores of HMCNs, which left much more room for the bilirubin molecules. Moreover, HMCNs showed high bilirubin-adsorption selectivity and low hemolytic effect. Therefore, HMCNs show potential utility for clinic hemoperfusion.

During hemoperfusion, the blood cells should freely and safely pass through the adsorption column. Therefore, millimeter-sized carbon spheres are desirable because of the large cavities between the spheres. Accordingly, we employed millimeter-sized mesoporous carbon spheres (MMCSs) for clinical bilirubin adsorption [47]. The MMCSs exhibited smooth surfaces and well-defined mesopores in the matrix. No obvious hemolytic and blood-coagulation effects were found after the co-incubation of MMCSs with RBCs and blood plasma, indicating the high blood compatibility of MMCSs. Importantly, MMCSs possessed high adsorption capacity towards bilirubin (148.4 mg g^{-1}). Their high adsorption capacity and desirable millimeter size make MMCSs a promising tool for clinical blood perfusion. We also demonstrated that magnetically functionalized HMCNs (M-HMCNs) with magnetic re-

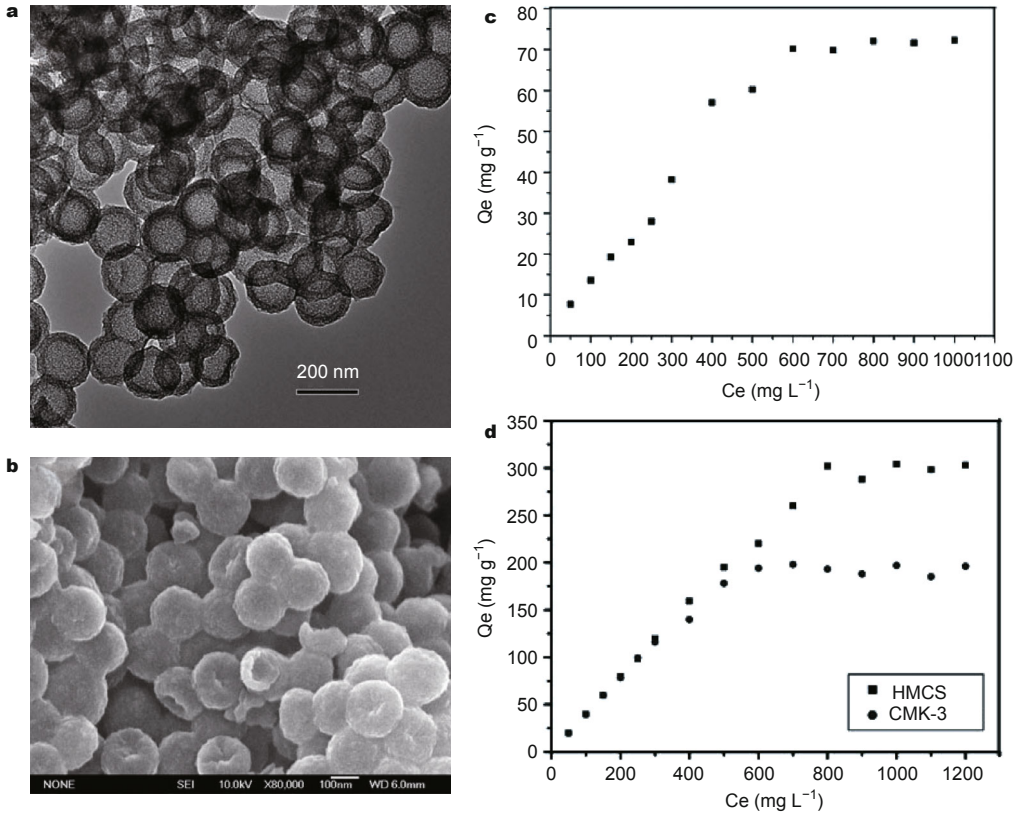

Figure 13 (a) TEM and (b) SEM images of as-synthesized HMCNs. Equilibrium adsorption isotherms of (c) active carbon and (d) CMK-3 and HMCNs. Reprinted with permission from Ref. [90]. Copyright 2009, Royal Society of Chemistry.

cycling capacity have potential use in bilirubin adsorption [92].

A mesoporous carbon monolith with controlled porosity is desirable for various applications, e.g., as the filling material in hemoperfusion. Therefore, we recently synthesized a mesoporous carbon monolith with hierarchical porosity from macro- to meso/microporosities and a cylindrical morphology determined by the container used (Figs 14a and b) for bilirubin adsorption [93]. The framework of the mesoporous carbon monolith features ordered mesoporosity, which was replicated directly from the mesoporous silica monolith used as the hard template, and the monolith showed negligible hemolytic effect (Fig. 14c). Importantly, the mesoporous carbon monolith had a high adsorption capacity for bilirubin (613 mg g^{-1}, Fig. 14d) compared to the adsorption capacity of active carbon (70 mg g^{-1}), CMK-3 mesoporous carbon (198 mg g^{-1}), and HMCNs (304 mg g^{-1}). A similar strategy for bilirubin adsorption using nitrogen-doped, hierarchically porous carbon was developed using natural banana peel as the carbon precursor [94].

MCBs can also be used in proteomics for disease diagnosis based on their high performance in peptide extraction

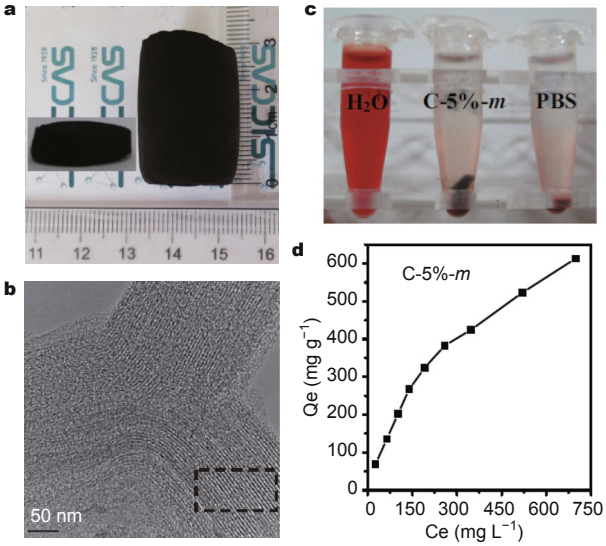

Figure 14 (a) Photograph of a cylindrical carbon monolith. (b) TEM image of the carbon monolith revealing the microstructure. (c) Hemolytic evaluation of the monolith using water as the positive control and phosphate buffered saline (PBS) as the negative control. (d) Adsorption isotherm of bilirubin using a carbon monolith adsorbent. Reprinted with permission from Ref. [93]. Copyright 2013, Elsevier.

from biological samples for mass spectrometry (MS) analysis. The hydrophobicity of carbon and the size-selective mesopores provide ordered mesoporous carbon (OMC) with high extraction and recovery capabilities for serum peptides (Fig. 15) [95]. Using OMC extraction and 2D LC-MS/MS analysis, Qin *et al.* [95] identified 3402 different endogenous peptides from 20 μL human serum, a much higher number than obtained with MCM-41 mesoporous silica. CMK-3 OMCs yielded high enrichment of N-linked glycans from serum samples due to size-exclusion [96]. In addition, M-HMCNs were designed and synthesized for rapid capture of low-abundance peptides from biosamples based on their high hydrophobicity and rapid magnetic response [97]. These results demonstrate that MCBs could be used for high-throughput screening of peptide biomarkers for disease diagnosis and treatment.

Because of their well-defined mesoporous structure, large surface area, good conductivity, and chemical stability, MCBs can be used to construct biosensing platforms. Pt-containing mesoporous carbon enhances the electron transfer and redox capability of glucose oxidase. Based on this principle, You *et al.* [98] designed a glucose biosensor with a low detection limit. 3D-ordered graphitized mesoporous carbon with 6-nm pores facilitated the improvement of pore-size-dependent enzymatic stability, bioactivity, and the direct electron transfer of entrapped enzymes, which were designed to detect hydrogen peroxide [99]. NiFex-embedded OMC provided a high-performance electrochemical biosensing platform for amperometric detection of hydrogen peroxide or glucose with high selectivity, high stability, and low interference [100]. Mesoporous carbon was also mixed with an ionic liquid (1-butyl-3-methylimidazolium hexafluorophosphate) and protein (glucose oxidase) as the microelectrode and demonstrated enhanced electrocatalytic activity and sensitivity and excellent stability for glucose biosensing [101].

Biocompatibility of MCBs

The biocompatibility of MSNs and several carbon-based biomaterials (e.g., carbon nanotubes and graphene) have been systematically investigated using several metrics, including biodistribution, excretion, biodegradation, histocompatibility, and hemocompatibility [102–107]. They have been demonstrated to be non-toxic at desirable doses. MCBs combine the mesoporous structure/spherical morphology of MSNs with the carbonaceous composition of graphene. Thus, it is anticipated that MCBs might be biocompatible. We recently presented *in vivo* long-term (30-day) histocompatibility results showing no effect of oxidized HMCNs on the main organs of mice (heart, liver, spleen, lung, and kidney) after intravenous injection of 20 mg kg^{-1} HMCNs. No apparent pathological changes were observed using the hematoxylin-eosin staining protocol [48]. Because they lack surface Si-OH, MCBs did not induce the RBC hemolysis observed for traditional mesoporous silica, indicating high hemocompatibility [47,90,93,94]. Although the preliminary biocompatibility results are encouraging, the biosafety evaluation of MCBs is still at the preliminary stage. The lack of general and adequate synthetic strategies to fabricate MCBs with highly desirable and reproducible structural/compositional parameters hinders the systematic evaluation of MCB biocompatibility. Biodegradation of MCBs is one of the most challenging future issues, similar to graphene and carbon nanotubes. Further rational structural design and compositional optimization of MCBs might provide strategies to solve this critical issue. Hence, the biocompatibility and biosafety of MCBs must be clarified as basic prerequisites for clinical translation.

CONCLUSIONS AND OUTLOOK

MCBs are considered the next generation of inorganic material systems for biomedical applications due to their com-

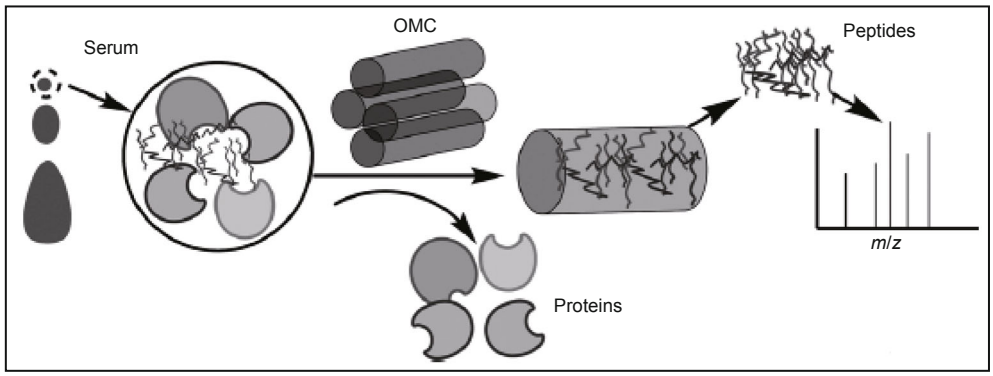

Figure 15 Schematic illustration of the enrichment of serum endogenous peptides by ordered mesoporous carbon (OMC). Reprinted with permission from Ref. [95]. Copyright 2011, WILEY-VCH Verlag GmbH & Co. KGaA.

bination of mesoporous nanostructure and carbonaceous composition. This review summarizes recent progress in the rational design, chemical construction, and biomedical applications of MCBs. Synthetic strategies for MCBs, especially spherical MCNs, such as nanocasting, soft-templating, and *in situ* framework transformation are discussed in detail. Due to their unique mesoporous structure, carbonaceous composition, and high biocompatibility, MCBs show high performance in controlled drug delivery/release, photothermal therapy, synergistic therapy, fluorescent labeling, bio-adsorption of toxic pathogenic substances, peptide separation, and biosensing. However, the biomedical applications of MCBs are still at the very early stage. Additional work is required to promote clinical translation of MCBs, as detailed below.

Scalable synthetic strategies for MCBs with optimized structural and compositional parameters for biomedicine are needed. To date, no general, controllable, and standard methodologies for obtaining MCBs have been developed, especially for size-tunable and hydrophilic spherical MCNs, and such methods are essential for biomedical applications.

Surface modification of MCBs remains challenging. Traditional oxidization of MCNs can endow the carrier with some specific organic groups for further modification, but the strong oxidization process partially destroys the carbonaceous framework and the mesostructure of MCBs, leading to structural collapse and reduced photothermal-conversion efficiency. Most importantly, surface modification is necessary to endow drug carriers with targeted drug delivery and sustained/controlled drug release functions, which, though extensively applied on MSNs, have been seldom used with MCBs.

In addition to drug delivery, traditional mesoporous silica-based biomaterials have been extensively applied for gene delivery, photodynamic therapy, antibacterial treatments, and even tissue engineering. Comparatively, MCBs have been explored in limited biomedical fields. MCBs are anticipated to show high performance in further biomedical areas due to their unique structure, composition, and physiochemical properties. Furthermore, use of MCNs in diagnostic imaging is rare compared to MSNs and graphene. MCNs with integrated functional modules are expected to provide diagnostic imaging functions for magnetic resonance imaging, ultrasonography, computed tomography, positron emission computed tomography, etc.

Systematic biosafety evaluations of MCBs are necessary to guarantee their clinical translation in the near future, and these evaluations will strongly depend on development of methods to obtain desirable MCBs. The biosafety evaluations should focus on the biodistribution, biodegradation, excretion, and other specific toxicities such as neurotoxicity, reproductive toxicity, and embryonic toxicity. Quantitative analysis of MCBs *in vivo* might be challenging because their carbonaceous composition will be influenced by carbon in living systems. Radiolabelling of MCBs might solve this issue for future biosafety evaluation.

In conclusion, we have reviewed the interdisciplinary research regarding the biomedical applications of MCBs, including chemistry, material science, biomedicine, and nano-biotechnology viewpoints. The preliminary results for MCBs and their promising performances in biomedicine are a bright prospect for the carbon-based biomaterial family, though their development is much slower than for carbon nanotubes, graphene, carbon dots, and fullerene. The structural features and high biomedical performances of MCBs demonstrate that optimization of chemical compositions beyond silica will endow mesoporous materials with unique characteristics unavailable to common mesoporous silica. However, many more pre-clinical evaluations are needed to promote the clinical translation of MCBs to benefit human health, and these will benefit from closer collaboration among researchers from different areas.

Received 29 January 2015; accepted 2 March 2015; published online 17 March 2015

1 Baughman RH, Zakhidov AA, de Heer WA. Carbon nanotubes—the route toward applications. Science, 2002, 297: 787–792
2 Allen MJ, Tung VC, Kaner RB. Honeycomb carbon: a review of graphene. Chem Rev, 2010, 110: 132–145
3 Liu Z, Robinson JT, Tabakman SM, Yang K, Dai HJ. Carbon materials for drug delivery & cancer therapy. Mater Today, 2011, 14: 316–323
4 Partha R, Conyers JL. Biomedical applications of functionalized fullerene-based nanomaterials. Int J Nanomed, 2009, 4: 261–275
5 Wang J, Hu Z, Xu J, Zhao Y. Therapeutic applications of low-toxicity spherical nanocarbon materials. NPG Asia Mater, 2014, 6: e84
6 Guo Y, Shi DL, Cho HS, *et al*. *In vivo* imaging and drug storage by quantum-dot-conjugated carbon nanotubes. Adv Funct Mater, 2008, 18: 2489–2497
7 Li RB, Wu R, Zhao L, *et al*. P-glycoprotein antibody functionalized carbon nanotube overcomes the multidrug resistance of human leukemia cells. ACS Nano, 2010, 4: 1399–1408
8 Liu Z, Fan AC, Rakhra K, *et al*. Supramolecular stacking of doxorubicin on carbon nanotubes for *in vivo* cancer therapy. Angew Chem Int Ed, 2009, 48: 7668–7672
9 Liu Z, Sun XM, Nakayama-Ratchford N, Dai HJ. Supramolecular chemistry on water-soluble carbon nanotubes for drug loading and delivery. ACS Nano, 2007, 1: 50–56
10 Liu Y, Hughes TC, Muir BW, *et al*. Water-dispersible magnetic carbon nanotubes as T2-weighted MRI contrast agents. Biomaterials, 2014, 35: 378–386
11 Liu Y, Hao X, Waddington LJ, Qiu J, Hughes TC. Surface modification of multiwalled carbon nanotubes with engineered self-assembled RAFT diblock coatings. Aus J Chem, 2014, 67: 151–158
12 Lim SY, Shen W, Gao ZQ. Carbon quantum dots and their applications. Chem Soc Rev, 2015, 44: 362–381
13 Zheng M, Liu S, Li J, *et al*. Integrating oxaliplatin with highly luminescent carbon dots: an unprecedented theranostic agent for personalized medicine. Adv Mater, 2014, 26: 3554–3560
14 Zhu S, Meng Q, Wang L, *et al*. Highly photoluminescent carbon

dots for multicolor patterning, sensors, and bioimaging. Angew Chem Int Ed, 2013, 52: 3953–3957
15 Chen Y, Xu P, Shu Z, *et al*. Multifunctional graphene oxide-based triple stimuli-responsive nanotheranostics. Adv Funct Mater, 2014, 24: 4386–4396
16 Chung C, Kim YK, Shin D, *et al*. Biomedical applications of graphene and graphene oxide. Acc Chem Res, 2013, 46: 2211–2224
17 Liu Z, Robinson JT, Sun XM, Dai HJ. PEGylated nanographene oxide for delivery of water-insoluble cancer drugs. J Am Chem Soc, 2008, 130: 10876–10877
18 Chen Y, Tan C, Zhang H, Wang L. Two-dimensional graphene analogues for biomedical applications. Chem Soc Rev, doi: 0.1039/C4CS00300D
19 Ku SH, Lee M, Park CB. Carbon-based nanomaterials for tissue engineering. Adv Healthc Mater, 2013, 2: 244–260
20 Yang K, Feng LZ, Shi XZ, Liu Z. Nano-graphene in biomedicine: theranostic applications. Chem Soc Rev, 2013, 42: 530–547
21 Chung C, Kim YK, Shin D, *et al*. Biomedical applications of graphene and graphene oxide. Acc Chem Res, 2013, 46: 2211–2224
22 Beg S, Rizwan M, Sheikh AM, *et al*. Advancement in carbon nanotubes: basics, biomedical applications and toxicity. J Pharm Pharmacol, 2011, 63: 141–163
23 Cha CY, Shin SR, Annabi N, Dokmeci MR, Khademhosseini A. Carbon-based nanomaterials: multifunctional materials for biomedical engineering. ACS Nano, 2013, 7: 2891–2897
24 Ambrogio MW, Thomas CR, Zhao YL, Zink JI, Stoddartt JF. Mechanized silica nanoparticles: a new frontier in theranostic nanomedicine. Acc Chem Res, 2011, 44: 903–913
25 Chen Y, Chen H, Shi J. *In vivo* bio-safety evaluations and diagnostic/therapeutic applications of chemically designed mesoporous silica nanoparticles. Adv Mater, 2013, 25: 3144–3176
26 Chen Y, Chen H, Shi J. Drug delivery/imaging multifunctionality of mesoporous silica-based composite nanostructures. Expert Opin Drug Deliv, 2014, 11: 917–930
27 Chen Y, Chen H, Shi J. Inorganic nanoparticle-based drug codelivery nanosystems to overcome the multidrug resistance of cancer cells. Mol Pharm, 2014, 11: 2495–2510
28 Chen Y, Meng Q, Wu M, *et al*. Hollow mesoporous organosilica nanoparticles: a generic intelligent framework-hybridization approach for biomedicine. J Am Chem Soc, 2014, 136: 16326–16334
29 Chen Y, Chen HR, Guo LM, *et al*. Hollow/rattle-type mesoporous nanostructures by a structural difference-based selective etching strategy. ACS Nano, 2010, 4: 529–539
30 Chen Y, Chen HR, Shi JL. Construction of homogenous/heterogeneous hollow mesoporous silica nanostructures by silica-etching chemistry: principles, synthesis, and applications. Acc Chem Res, 2014, 47: 125–137
31 Chen Y, Chu C, Zhou YC, *et al*. Reversible pore-structure evolution in hollow silica nanocapsules: large pores for sirna delivery and nanoparticle collecting. Small, 2011, 7: 2935–2944
32 Wu SH, Hung Y, Mou CY. Mesoporous silica nanoparticles as nanocarriers. Chem Commun, 2011, 47: 9972–9985
33 Mamaeva V, Sahlgren C, Linden M. Mesoporous silica nanoparticles in medicine-recent advances. Adv Drug Deliv Rev, 2013, 65: 689–702
34 Tang FQ, Li LL, Chen D. Mesoporous silica nanoparticles: synthesis, biocompatibility and drug delivery. Adv Mater, 2012, 24: 1504–1534
35 Shi JL, Chen Y, Chen HR. Progress on the multifunctional mesoporous silica-based nanotheranostics. J Inorg Mater, 2013, 28: 1–11
36 Ryoo R, Joo SH, Kruk M, Jaroniec M. Ordered mesoporous carbons. Adv Mater, 2001, 13: 677–681
37 Liang CD, Li ZJ, Dai S. Mesoporous carbon materials: synthesis and modification. Angew Chem Int Ed, 2008, 47: 3696–3717
38 Kim TW, Chung PW, Slowing II, *et al*. Structurally ordered mesoporous carbon nanoparticles as transmembrane delivery vehicle in human cancer cells. Nano Lett, 2008, 8: 3724–3727
39 Gu JL, Su SS, Li YS, He QJ, Shi JL. Hydrophilic mesoporous carbon nanoparticles as carriers for sustained release of hydrophobic anti-cancer drugs. Chem Commun, 2011, 47: 2101–2103
40 Sun Z, Liu Y, Li B, *et al*. General synthesis of discrete mesoporous carbon microspheres through a confined self-assembly process in inverse opals. ACS Nano, 2013, 7: 8706–8714
41 Liang CD, Hong KL, Guiochon GA, Mays JW, Dai S. Synthesis of a large-scale highly ordered porous carbon film by self-assembly of block copolymers. Angew Chem Int Ed, 2004, 43: 5785–5789
42 Zhang F, Gu D, Yu T, *et al*. Mesoporous carbon single-crystals from organic-organic self-assembly. J Am Chem Soc, 2007, 129: 7746–7747
43 Fang Y, Gu D, Zou Y, *et al*. A low-concentration hydrothermal synthesis of biocompatible ordered mesoporous carbon nanospheres with tunable and uniform size. Angew Chem Int Ed, 2010, 49: 7987–7991
44 Liu J, Yang T, Wang DW, *et al*. A facile soft-template synthesis of mesoporous polymeric and carbonaceous nanospheres. Nat Commun, 2013, 4: 2798
45 Tang J, Liu J, Li C, *et al*. Synthesis of nitrogen-doped mesoporous carbon spheres with extra-large pores through assembly of diblock copolymer micelles. Angew Chem Int Ed, 2015, 54: 588–593
46 Li M, Xue J. Ordered mesoporous carbon nanoparticles with well-controlled morphologies from sphere to rod via a soft-template route. J Colloid Interface Sci, 2012, 377: 169–175
47 Guo LM, Zhang JM, He QJ, *et al*. Preparation of millimetre-sized mesoporous carbon spheres as an effective bilirubin adsorbent and their blood compatibility. Chem Commun, 2010, 46: 7127–7129
48 Chen Y, Xu P, Wu M, *et al*. Colloidal RBC-shaped, hydrophilic, and hollow mesoporous carbon nanocapsules for highly efficient biomedical engineering. Adv Mater, 2014, 26: 4294–4301
49 Chen Y, Xu PF, Chen HR, *et al*. Colloidal HPMO nanoparticles: silica-etching chemistry tailoring, topological transformation, and nano-biomedical applications. Adv Mater, 2013, 25: 3100–3105
50 Qiao ZA, Guo BK, Binder AJ, *et al*. Controlled synthesis of mesoporous carbon nanostructures via a "silica-assisted" strategy. Nano Lett, 2013, 13: 207–212
51 Zhu J, Liao L, Bian XJ, *et al*. pH-controlled delivery of doxorubicin to cancer cells, based on small mesoporous carbon nanospheres. Small, 2012, 8: 2715–2720
52 Zhou L, Dong K, Chen Z, Ren J, Qu X. Near-infrared absorbing mesoporous carbon nanoparticle as an intelligent drug carrier for dual-triggered synergistic cancer therapy. Carbon, 2015, 82: 479–488
53 Xu G, Liu S, Niu H, Lv W, Wu R. Functionalized mesoporous carbon nanoparticles for targeted chemo-photothermal therapy of cancer cells under near-infrared irradiation. RSC Adv, 2014, 4: 33986–33997
54 Zhu S, Chen C, Chen Z, *et al*. Thermo-responsive polymer-functionalized mesoporous carbon for controlled drug release. Mater Chem Phys, 2011, 126: 357–363
55 Lu J, Liong M, Zink JI, Tamanoi F. Mesoporous silica nanoparticles as a delivery system for hydrophobic anticancer drugs. Small, 2007, 3: 1341–1346
56 Saha D, Warren KE, Naskar AK. Controlled release of antipyrine from mesoporous carbons. Microporous Mesoporous Mat, 2014, 196: 327–334
57 Schornack PA, Gillies RJ. Contributions of cell metabolism and H^+ diffusion to the acidic pH of tumors. Neoplasia, 2003, 5: 135–145
58 Crayton SH, Tsourkas A. pH-titratable superparamagnetic iron oxide for improved nanoparticle accumulation in acidic tumor microenvironments. ACS Nano, 2011, 5: 9592–9601
59 Chen Y, Ye D, Wu M, *et al*. Break-up of two-dimensional MnO_2 nanosheets promotes ultrasensitive pH-triggered theranostics of

cancer. Adv Mater, 2014, 26: 7019–7026
60 Chen Y, Yin Q, Ji XF, *et al*. Manganese oxide-based multifunctionalized mesoporous silica nanoparticles for pH-responsive MRI, ultrasonography and circumvention of MDR in cancer cells. Biomaterials, 2012, 33: 7126–7137
61 Chen Y, Chen HR, Sun Y, *et al*. Multifunctional mesoporous composite nanocapsules for highly efficient MRI-guided high-intensity focused ultrasound cancer surgery. Angew Chem Int Ed, 2011, 50: 12505–12509
62 Wang X, Chen HR, Chen Y, *et al*. Perfluorohexane-encapsulated mesoporous silica nanocapsules as enhancement agents for highly efficient high intensity focused ultrasound (HIFU). Adv Mater, 2012, 24: 785–791
63 Chen Y, Chen H, Shi J. Nanobiotechnology promotes noninvasive high-intensity focused ultrasound cancer surgery. Adv Healthc Mater, 2015, 4: 158–165
64 Fang Y, Zheng G, Yang J, *et al*. Dual-pore mesoporous carbon@silica composite core-shell nanospheres for multidrug delivery. Angew Chem Int Ed, 2014, 53: 5366–5370
65 Zhu W, Zhao Q, Zheng X, *et al*. Mesoporous carbon as a carrier for celecoxib: the improved inhibition effect on MDA-MB-231 cells migration and invasion. Asian J Pharm Sci, 2014, 9: 82–91
66 Wang T, Zou M, Jiang H, *et al*. Synthesis of a novel kind of carbon nanoparticle with large mesopores and macropores and its application as an oral vaccine adjuvant. Eur J Pharm Sci, 2011, 44: 653–659
67 Wang X, Pan Y, Wang J, Tian Y. Synthesis of magnetic dual-mesoporous carbon spheres and lysozyme release behavior. Micropor Mesopor Mat, 2013, 180: 257–261
68 Robinson JT, Tabakman SM, Liang YY, *et al*. Ultrasmall reduced graphene oxide with high near-infrared absorbance for photothermal therapy. J Am Chem Soc, 2011, 133: 6825–6831
69 Tian B, Wang C, Zhang S, Feng LZ, Liu Z. Photothermally enhanced photodynamic therapy delivered by nano-graphene oxide. ACS Nano, 2011, 5: 7000–7009
70 Feng LY, Wu L, Qu XG. New horizons for diagnostics and therapeutic applications of graphene and graphene oxide. Adv Mater, 2013, 25: 168–186
71 Hu SH, Chen YW, Hung WT, Chen IW, Chen SY. Quantum-dot-tagged reduced graphene oxide nanocomposites for bright fluorescence bioimaging and photothermal therapy monitored *in situ*. Adv Mater, 2012, 24: 1748–1754
72 Markovic ZM, Harhaji-Trajkovic LM, Todorovic-Markovic BM, *et al*. *In vitro* comparison of the photothermal anticancer activity of graphene nanoparticles and carbon nanotubes. Biomaterials, 2011, 32: 1121–1129
73 Wang Y, Wang K, Yan X, Huang R. A general strategy for dual-triggered combined tumor therapy based on template semi-graphitized mesoporous silica nanoparticles. Adv Healthc Mater, 2014, 3: 485–489
74 Wang Y, Wang K, Zhang R, *et al*. Synthesis of core-shell graphitic carbon@silica nanospheres with dual-ordered mesopores for cancer-targeted photothermochemotherapy. ACS Nano, 2014, 8: 7870–7879
75 Wang L, Sun Q, Wang X, *et al*. Using hollow carbon nanospheres as a light-induced free radical generator to overcome chemotherapy resistance. J Am Chem Soc, 2015, 137: 1947–1955
76 Li H, Kang Z, Liu Y, Lee ST. Carbon nanodots: synthesis, properties and applications. J Mater Chem, 2012, 22: 24230–24253
77 Li L, Wu G, Yang G, *et al*. Focusing on luminescent graphene quantum dots: current status and future perspectives. Nanoscale, 2013, 5: 4015–4039
78 Luo PG, Sahu S, Yang ST, *et al*. Carbon "quantum" dots for optical bioimaging. J Mater Chem B, 2013, 1: 2116–2127
79 Chen B, Li F, Li S, *et al*. Large scale synthesis of photoluminescent carbon nanodots and their application for bioimaging. Nanoscale, 2013, 5: 1967–1971
80 Ding C, Zhu A, Tian Y. Functional surface engineering of C-dots for fluorescent biosensing and *in vivo* bioimaging. Acc Chem Res, 2014, 47: 20–30
81 Cui Y, Hu Z, Zhang C, Liu X. Simultaneously enhancing up-conversion fluorescence and red-shifting down-conversion luminescence of carbon dots by a simple hydrothermal process. J Mater Chem B, 2014, 2: 6947–6952
82 Chen H, Wang GD, Tang W, *et al*. Gd-encapsulated carbonaceous dots with efficient renal clearance for magnetic resonance imaging. Adv Mater, 2014, 26: 6761–6766
83 Kong Q, Zhang L, Liu J, *et al*. Facile synthesis of hydrophilic multi-colour and upconversion photoluminescent mesoporous carbon nanoparticles for bioapplications. Chem Commun, 2014, 50: 15772–15775
84 He QJ, Ma M, Wei CY, Shi JL. Mesoporous carbon@silicon-silica nanotheranostics for synchronous delivery of insoluble drugs and luminescence imaging. Biomaterials, 2012, 33: 4392–4402
85 Duffy P, Magno LM, Yadav RB, *et al*. Incandescent porous carbon microspheres to light up cells: solution phenomena and cellular uptake. J Mater Chem, 2012, 22: 432–439
86 Dong Y, Lin H, Jin Q, *et al*. Synthesis of mesoporous carbon fibers with a high adsorption capacity for bulky dye molecules. J Mater Chem A, 2013, 1: 7391–7398
87 Liu Y, Wu Z, Chen X, *et al*. A hierarchical adsorption material by incorporating mesoporous carbon into macroporous chitosan membranes. J Mater Chem, 2012, 22: 11908–11911
88 Dong Y, Lin HM, Qu FY. Synthesis of ferromagnetic ordered mesoporous carbons for bulky dye molecules adsorption. Chem Eng J, 2012, 193: 169–177
89 Zhuang X, Wan Y, Feng CM, Shen Y, Zhao DY. Highly efficient adsorption of bulky dye molecules in wastewater on ordered mesoporous carbons. Chem Mater, 2009, 21: 706–716
90 Guo LM, Zhang LX, Zhang JM, *et al*. Hollow mesoporous carbon spheres-an excellent bilirubin adsorbent. Chem Commun, 2009: 6071–6073
91 Kamisako T, Kobayashi Y, Takeuchi K, *et al*. Recent advances in bilirubin metabolism research: the molecular mechanism of hepatocyte bilirubin transport and its clinical relevance. J Gastroenterol, 2000, 35: 659–664
92 Guo LM, Cui XZ, Li YS, *et al*. Hollow mesoporous carbon spheres with magnetic cores and their performance as separable bilirubin adsorbents. Chem Asian J, 2009, 4: 1480–1485
93 Tao G, Zhang L, Hua Z, *et al*. Highly efficient adsorbents based on hierarchically macro/mesoporous carbon monoliths with strong hydrophobicity. Carbon, 2014, 66: 547–559
94 Liu RL, Ji WJ, He T, *et al*. Fabrication of nitrogen-doped hierarchically porous carbons through a hybrid dual-template route or CO_2 capture and haemoperfusion. Carbon, 2014, 76: 84–95
95 Qin H, Gao P, Wang F, *et al*. Highly efficient extraction of serum peptides by ordered mesoporous carbon. Angew Chem Int Ed, 2011, 50: 12218–12221
96 Qin H, Zhao L, Li R, Wu Ra, Zou H. Size-selective enrichment of N-linked glycans using highly ordered mesoporous carbon material and detection by MALDI-TOF MS. Anal Chem, 2011, 83: 7721–7728
97 Cheng G, Zhou MD, Zheng SY. Facile synthesis of magnetic mesoporous hollow carbon microspheres for rapid capture of low-concentration peptides. ACS Appl Mater Inter, 2014, 6: 12719–12728
98 You C, Li X, Zhang S, *et al*. Electrochemistry and biosensing of glucose oxidase immobilized on Pt-dispersed mesoporous carbon. Microchimica Acta, 2009, 167: 109–116
99 Lu X, Xiao Y, Lei Z, *et al*. A promising electrochemical biosensing platform based on graphitized ordered mesoporous carbon. J Mater Chem, 2009, 19: 4707–4714

100 Xiang D, Yin L, Ma J, *et al*. Amperometric hydrogen peroxide and glucose biosensor based on $NiFe_2$/ordered mesoporous carbon nanocomposites. Analyst, 2015, 140: 644–653
101 Sun W, Guo CX, Zhu Z, Li CM. Ionic liquid/mesoporous carbon/protein composite microelectrode and its biosensing application. Electrochem Commun, 2009, 11: 2105–2108
102 He QJ, Shi JL, Zhu M, Chen Y, Chen F. The three-stage *in vitro* degradation behavior of mesoporous silica in simulated body fluid. Micropor Mesopor Mat, 2010, 131: 314–320
103 He QJ, Zhang ZW, Gao F, Li YP, Shi JL. *In vivo* biodistribution and urinary excretion of mesoporous silica nanoparticles: effects of particle size and PEGylation. Small, 2011, 7: 271–280
104 Huang XL, Li LL, Liu TL, *et al*. The shape effect of mesoporous silica nanoparticles on biodistribution, clearance, and biocompatibility *in vivo*. ACS Nano, 2011, 5: 5390–5399
105 Chung TH, Wu SH, Yao M, *et al*. The effect of surface charge on the uptake and biological function of mesoporous silica nanoparticles 3T3-L1 cells and human mesenchymal stem cells. Biomaterials, 2007, 28: 2959–2966
106 Hudson SP, Padera RF, Langer R, Kohane DS. The biocompatibility of mesoporous silicates. Biomaterials, 2008, 29: 4045–4055
107 Li ZX, Barnes JC, Bosoy A, Stoddart JF, Zink JI. Mesoporous silica nanoparticles in biomedical applications. Chem Soc Rev, 2012, 41: 2590–2605

Acknowledgements This research was supported by the National Natural Science Foundation of China (51302293 and 51132009), Natural Science Foundation of Shanghai (13ZR1463500), Shanghai Rising-Star Program (14QA1404100), and Youth Scholar of State Key Laboratory of High Performance Ceramics and Superfine Microstructures (SKL201203).

Author contributions Y. Chen and J. Shi wrote the manuscript together.

Conflict of interest The authors declare that they have no conflict of interest.

Yu Chen received his BSc degree at Nanjing Tech University and PhD degree at Shanghai Institute of Ceramics, Chinese Academy of Sciences (SICCAS). He is now an associate professor at SICCAS. His research includes the design, synthesis, and biomedical applications of zero-dimensional mesoporous materials, two-dimensional nanosheets, and three-dimensional implants, including mesoporous materials for drug delivery, molecular probes for molecular imaging, ultrasound therapy, non-viral gene delivery vehicles, and *in situ* localized tumor therapy.

Jianlin Shi received his PhD degree at SICCAS. He is now a professor at SICCAS. His research areas include synthesis of mesoporous materials and mesoporous-based nano-composites and their catalytic, biomedical, and optical applications. He has published over 300 scientific papers with over 12,000 citations by other scientists and an h-index of 57 (2014). He has overseen more than 30 important research projects and has gained a number of awards for his achievements.

中文摘要 纳米生物技术为重大疾病的精确诊断和高效治疗提供了全新、高效和多样化的途径. 新型生物材料体系的开发是实现纳米生物技术临床转化、病人个人化治疗、从而造福病人的关键要素之一. 作为新的无机材料体系, 介孔碳生物材料(MCBs)结合了介孔纳米结构和碳组成的优点, 与介孔氧化硅和碳基纳米材料(如石墨烯、碳纳米管、富勒烯)相比, 在生物医学领域展现出更多的优点. 这篇综述重点阐述了MCBs的设计、化学合成以及在生物医学领域中的应用进展. 论文首先总结了MCBs, 特别是介孔碳纳米颗粒(MCNs)的制备方法. 随后详细地综述了MCBs在可控药物释放、光热治疗、协同治疗、荧光细胞标记、人体有毒物质的生物吸附、肽分离和生物传感中的应用. 在此基础上, 初步讨论了MCBs的生物安全性. 由于MCBs具有特殊的纳米结构、化学组成和良好的生物相容性, 一旦目前MCBs面临的几个难题得到圆满解决, 我们有理由相信其在不久的将来会实现临床转化和应用.